Design and experiment of pneumatic seed clearing mechanism for pin-hole tube wheat plot precision sowing device

Xirui Zhang[1,3], Youming Yang[1], Qingjie Wang[2], Hongwen Li[2], Zhifu Zhang[1], Junxiao Liu[1,3*]

(1. *School of Mechanical and Electrical Engineering, Hainan University, Haikou 570228, China*;
2. *College of Engineering, China Agricultural University, Beijing 100083, China*;
3. *Sanya Nanfan Research Institute of Hainan University, Sanya 572025, Hainan, China*)

Abstract: For the problem that when wheat is sucked up by the air suction method, the seeds are aligned in a small area, making it difficult for the contact seed cleaning mechanism to clean the seeds. The mechanism of seed cleaning airflow on wheat seed was studied, the flow velocity distribution relationship of the jet section was defined, the mathematical model of the jet velocity of circular and plane sections was established, and the key factors that could have a significant influence on seed cleaning effect were explored. A non-contact positive pressure air flow seed cleaning method was proposed. After theoretical calculations, it is concluded that the core section lengths of the circular section jet and the inline jet are 24.8 mm and 28.8 mm, respectively. The clearing distance is set to 20 mm. Through the single-factor test, the best air tube nozzle shape was clarified as a vertical inline nozzle. The angle of seed cleaning, the air velocity of seed cleaning, and the negative supply pressure were selected as influencing factors, and the seed leakage index, seed reabsorption index, and seed qualification index as the evaluation indicators to conduct a 3-factor 5-horizontal rotation test. A mathematical regression model of influencing factors and evaluation indexes was established to analyze the influence of these factors and indexes. The optimal operation parameters were obtained as the seed cleaning Angle of 19°, the seed cleaning air velocity of 58 m/s, and the negative pressure of 8.5 kPa. Under the optimal parameters, the seed leakage suction index is 8.23%, the seed reabsorption index is 0.33%, and the seed qualification index is 91.44%, which meets the design requirements.

Keywords: wheat, precision seed-metering device, clearing, seed, positive pressure airflow, jet flow field
DOI: 10.25165/j.ijabe.20231604.8006

Citation: Zhang X R, Yang Y M, Wang Q J, Li H W, Zhang Z F, Liu J X. Design and experiment of pneumatic seed clearing mechanism for pin-hole tube wheat plot precision sowing device. Int J Agric & Biol Eng, 2023; 16(4): 85–95.

1 Introduction

As one of the three staple grains in China, Wheat plays an important role in maintaining China's food security[1,2]. High-quality seed varieties are significant in ensuring high and stable wheat yield. According to statistics, in developed countries, the comprehensive contribution of superior seed varieties to agricultural production growth can be as high as 50%[3,4]. Agronomists must carry out large-scale field breeding experiments[5] to cultivate superior seeds. The requirement for sowing precision is especially strict in the original seed production period (plant row or ear row stage). Both re-sowing and miss-sowing will significantly impact the accuracy and reliability of the breeding test[6].

Seed clearing refers to ensuring that only one seed is in each hole of the seed sowing machine by clearing out the excess seeds with external intervention or the weight of the seed itself (single precision seed metering device). It is a crucial method to ensure the single-seed rate of the seed-sowing machine[7-9]. The pinhole wheeled wheat plot single-seed precision sowing machine[10,11] developed in the previous stage may cause miss sowing. Since its absorption device is outside the machine, the drag force is the only force on seeds, making it easy to clear out all the adsorbed seeds by the contact clearing method. Therefore, the non-contact clearing method is put forward as an effective way to ensure the single-seed rate.

The research on single-seed precision sowing machines applied in wheat plots in developed countries started earlier[12-15]. As a typical seed sowing device, made by Wintersteiger Company[16], the air suction spirally grooved plate precision sowing device uses the displacement generated by the relative rotation of the radial groove and the spiral groove to remove the excess seeds adsorbed, obtaining a higher single-seed rate[17]. Also, a dibbling machine in foreign countries is of high price and complex and precise structure, which is unsuitable for application in a small-sized seeding machine. There is a shortage of single-grain precision sowing machinery in wheat plots in China, which has become the bottleneck and critical link in wheat variety testing. The shortage of mechanized fine sowing reduces the launch efficiency of new wheat varieties but also affects the rapid and healthy development of the wheat breeding industry. Regarding single-seed dibbling, instead of the traditional seed-sowing device, Zhang et al.[18,19] adopted PLC technology to control a pneumatic manipulator, which improved the sowing accuracy in breeding. The drum-type air-auction vegetable seedling planter was designed by Liu et al.[20-22] adopts dual- nozzle

Received date: 2022-10-31 **Accepted date:** 2023-05-24
Biographies: **Xirui Zhang**, PhD, Professor, research interest: modern agricultural equipment, Email: zhangxirui_999@sina.com; **Youming Yang**, master candidate, research interest: seeding equipment, Email: 3261000199@qq.com; **Qingjie Wang**, PhD, Professor, research interest: conservation tillage and equipment, Email: wangqingjie@cau.edu.cn; **Hongwen Li**, PhD, Professor, research interest: conservation tillage agriculture equipment engineering. Email: lhwen@cau.edu.cn; **Zhifu Zhang**, PhD, Associate Professor, research interest: mechanical equipment and vibration, Email: jeff.zfzhang@foxmail.com.
***Corresponding author: Junxiao Liu**, PhD, Lecturer, research interest: modern agricultural equipment. School of Mechanical and Electrical Engineering, Hainan University, No.58 Renmin Avenue, Meilan District, Haikou 570228, China. Tel: +86-18811762707, Email: 995229@hainanu.edu.cn.

system to clean the area around the suction nozzle, which can effectively clean up the excess seeds entrained. Zhang et al.[23,24] designed an air nozzle for seed clearing, set up a mathematical model for the seed clearing process, and optimized the optimal wind pressure value in seed clearing. To solve the problems of high energy consumption and low efficiency (single row sowing) when a precision sowing machine was adopted to sow cotton seeds, Ni et al.[25,26] adopted an array of suction holes to suck seeds and a lateral air-cleaning device to clear seeds. The above studies have explored and proved the feasibility of air-blowing for seed clearing. Still, the seeds sucking in the devices above are far different from that in pinhole wheeled wheat plot single-seed precision sowing device.

Taking the pinhole wheeled wheat plot single-seed precision sowing device as the research object, this paper studies the clearing efficacy of positive airflow on adsorbed seeds, defines the velocity distribution of jet cross-section, explores the effect of seed clearing airflow and the key factors that can significantly affect the seed clearing, establishes a mathematical model of jet velocity for cross-sections in different shape, and optimize the seed clearing parameters, to reduce re-sowing, avoid false clearing and achieve single-seed separation, laying a foundation for the development and manufacture of high precision plot breeding machine.

2 Design of pinhole wheeled wheat plot precision single-seed sowing device

2.1 Overall structural design

The pinhole wheeled wheat plot precision sowing device mainly comprises a storage battery, walking tractor, DC fan, frame, automatic seed supply device, pneumatic pinhole wheel type single-seed precision sowing device, pressing wheel, etc. The overall structure is shown in Figure 1.

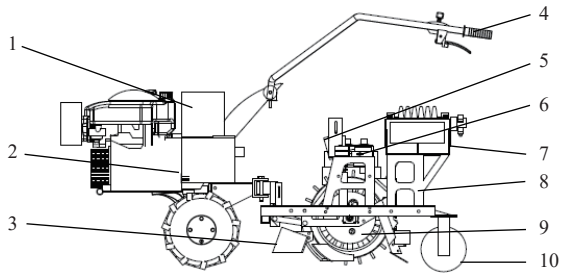

1. Accumulator battery 2. Walking tractor 3. Flat soil slab 4. Pushrod 5. Lifting mechanism 6. DC fan 7. Automatic seed supply mechanism 8. Rack 9. Pinhole wheel type single grain precision seeding device 10. Suppression of wheel

Figure 1 Pinhole tube wheat plot single-seed machine

Powered by a walking tractor, with its DC fan powered by a storage battery, the single-seed precision seeder adopts a push rod to control the travel direction, which can bend and turn and reduce the turning radius. When working in the field, the single-seed precision sowing machine can successively complete soil levelling, trenching, single-seed precision sowing, soil covering, soil compaction, etc.

The power of the seeding device comes from the ground wheel coaxial with the pinhole wheel, which can obtain the machine's forward speed and ensure the plant spacing. The automated seed supply device can fill the seed hopper with a specified quantity for each plot, controlled by a step motor with a one-key operation. Lift the unloading handle, place it in the card slot, and keep the unloading cover of the seed hopper open to unload the remaining seeds that will be unloaded into the recycling box under the vibration caused by the rotation of the pinhole wheel. Turn the unloading handle back and close the seed hopper when the unloading cover is automatically returned to the original position to start a new seed supply for another plot.

2.2 Working principle of sowing device

The seed suction holes are uniformly distributed on the outer wall of the pinhole wheel that is closely coordinated with the pneumatic distribution cover, as shown in Figure 2. The counter-rotating of the wheel and the cover control the switch of positive and negative pressure. The seed hopper with seed-clearing air pipes connected is installed above the pinhole wheel. Blew by the positive pressure airflow, the excess seeds on the seed suction hole are removed back to the seed hopper. Before covering the soil, the pinhole wheel will be put in the furrow with the seed suction hole closely contacting the seed bed to fling seeds. The positive pressure airflow will clean the seed suction hole to prevent blockage.

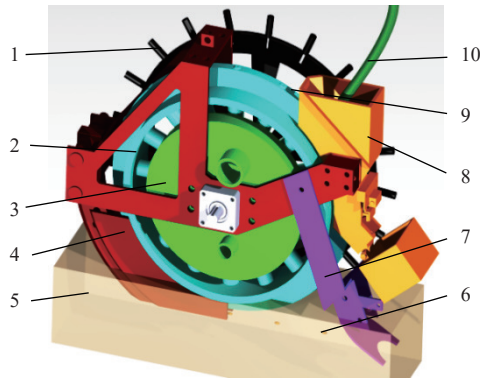

1. Earth wheel 2. Pinhole wheel 3. Force distribution cover 4. Trenching mechanism 5. Soil 6. Seed 7. The soil covering mechanism 8. Seed box 9. Seed suction hole 10. Seed cleaning mechanism

Figure 2 Schematic diagram of the sowing device structure

3 Study on the jet flow of seed-clearing air-pipe

The pretest of the precision sowing device showed that multiple suction and missed suction are mutually exclusive. That is, the miss suction can be avoided while multiple suction cannot meet the requirement when the negative supply pressure is significant; In contrast, multiple suction is avoided when decreasing the negative supply pressure and missed suction occurs significantly increase. Worse, no such negative pressure can ensure proper multiple suction and missed suction. Therefore, sucking with a high negative pressure to ensure the seed absorption rate while adopting an appropriate seed-clearing method to remove the excess seeds is an effective way to increase the single-seed rate.

3.1 Study on seed stress

The positive pressure flow from the seed-clearing air pipe is free to submerge jets[27] from a closed pressure chamber into infinite broad space with a uniform medium. After the seed adsorption hole adsorbs the seed, the force of airflow on the seed is the critical fain breaking break the seed adsorption equilibrium, and the seed is subjected to the air-blowing force[28] as

$$F_b = \frac{C\rho S V^2}{2} \quad (1)$$

where, F_b is the air blowing force on the seed, N; C is the air resistance coefficient; ρ is the air density, kg/m^3; S is the upwind area of seeds, m^2; V is the relative velocity of seed and airflow, m/s.

From Equation (1), the blowing force of positive pressure airflow on seeds is mainly related to the relative movement velocity between seeds and airflow and the upwind area of seeds. The upwind area mainly depends on the adsorption forms of seeds,

which is challenging to be artificially controlled. The relative motion velocity between seeds and airflow is the resultant velocity generated by the relative motion between the circular motion of the seeds rotating with the pinhole wheel and the positive pressure air velocity. In operation, the linear speed at the seed suction hole of the pinhole wheel is equal to the machine's forward speed generally, 1-1.5 km/h in plot operation. Therefore, the flow velocity of positive pressure airflow is the critical factor determining seeds' air-blowing force value rally. Reynolds number *Re* is applied to describe the property of positive pressure airflow. The critical Reynolds number of the jet outlet is defined as follows:

$$Re = \frac{d_0 u_0}{v} \tag{2}$$

where, d_0 is the characteristic length of the jet outlet, m; u_0 is the average flow velocity of the jet outlet, m/s; v is the kinematic viscosity coefficient, m^2/s.

When the characteristic length is 0.004 m, calculated according to the diameter of the round nozzle, and the measured average velocity at the outlet of the jet is 50 m/s kinematic viscosity coefficient will be

$$v = \frac{\mu}{\rho} \tag{3}$$

where, μ is the kinematic viscosity coefficient, N·s /m^2.

Under standard conditions, the air density is about 1.29 kg/m^3, and the kinematic viscosity coefficient is 17.9×10^{-6} N·s/m^2. Then the Reynolds number at the outlet of the jet of clearing air pipe is about 13 464. According to the literature[29], a jet with a Reynolds number more significant than the critical value of 2300 can be defined as turbulence, also known as a turbulent jet.

Due to the turbulent characteristics of the high-speed jet, airflow entrains and moves forward with the surrounding air, causing an expansion of the jet cross-section and an increase in the flow rate[30]. The boundary is shown as an irregular surface composed of interlacing. To simplify the calculation, the boundary is approximated as a straight line by average statistical significance.

The diagram of jet distribution is shown in Figure 3. The stroke of the jet can be roughly divided into the initial section and the main section. The initial section contains the core area of the airflow, in which the air is pure without any mix of outside air. The initial airflow in the tube is of high velocity and decreases with the increase of the jet stroke. With continuous attenuation, it disappears when it enters the core area. Then the jet flow enters the central section[31-34].

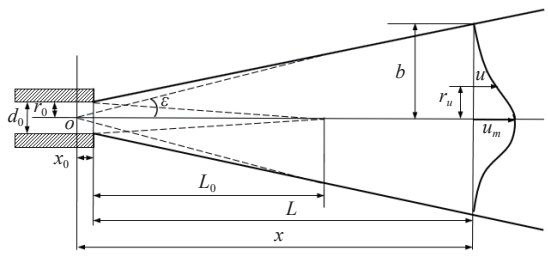

Note: d_0 is the characteristic length of the pipe mouth, mm; L_0 is the length of the initial section, mm; L is the jet stroke outside the tube, mm; O is the jet pole; x_0 is the distance from the jet pole to the pipe mouth, mm; x is the length of the jet, mm; r_0 is half of the characteristic length of the pipe mouth, mm; b is the jet width, mm; ε is the expansion angle of the central section, (°); r_u is the distance from the centerline to any other point, mm; u is the velocity of airflow at any point, m/s; u_m is the centerline airflow velocity, m/s。

Figure 3 Schematic diagram of jet distribution

3.2 Study on the influence of nozzle shape on the airflow velocity

At the same flow rate in a closed pipeline, airflow velocity increases while reducing the cross-section. Thus, it is an effective way to increase the flow rate by adding a small nozzle at the end of the air pipe. Conical nozzles and inline nozzles are commonly used[35]. When the momentum conservation equation is established for each section of the jet, the momentum conservation equation of the jet on the circular cross-section is obtained[36].

$$\delta\rho v_0^2 \pi {r_0}^2 = \int_0^b \rho u^2 2\pi r_u \mathrm{d}r_u \tag{4}$$

where, δ is the momentum correction coefficient of the outlet section; v_0 is the average velocity of airflow at the mouth of the pipe, m/s.

Both sides of the equation are divided by $2\rho bum^2$; the following equation is obtained.

$$\delta\left(\frac{r_0}{b}\right)^2\left(\frac{v_0}{u_\mathrm{m}}\right)^2 = 2\int_0^1 \left(\frac{u}{u_\mathrm{m}}\right)^2 \frac{r_u}{b}\mathrm{d}\frac{r_u}{b} \tag{5}$$

The momentum conservation equation of the jet on the inline cross-section is

$$\rho v_0^2 2r_0 = 2\int_0^b \rho u^2 \mathrm{d}r_u \delta \tag{6}$$

It is as follows when both sides are divided by $2\rho bum^2$

$$\left(\frac{v_0}{u_\mathrm{m}}\right)^2 \frac{\delta r_0}{b} = \int_0^1 \left(\frac{u}{u_\mathrm{m}}\right)^2 \mathrm{d}\frac{r_u}{b} \tag{7}$$

According to experimental data[37], the velocity distribution of jets on the circular cross-section and the inline section is

$$\frac{u}{u_\mathrm{m}} = \left[1-\left(\frac{r_u}{b}\right)^{1.5}\right]^2 \tag{8}$$

From the geometric relationship in Figure 3, the jet width b is

$$b = (x_0 + L)\tan\varepsilon \tag{9}$$

Suppose η is equal to r_u/b, with Equations (8) and (9) substituted in Equations (5) and (7), respectively; the jet velocities of the circular section and inline section are obtained

$$u_\mathrm{mc} = \frac{v_0 r_0}{(x_0+L)\tan\varepsilon}\sqrt{\frac{\delta}{2\int_0^1\left[\left(1-(\eta)^{1.5}\right)^2\right]^2\eta d\eta}} \tag{10}$$

$$u_\mathrm{mp} = \sqrt{\frac{\delta r_0}{(x_0+L)\tan\alpha\int_0^1\left[\left(1-(\eta)^{1.5}\right)^2\right]^2 d\eta}}v_0 \tag{11}$$

where, u_mc is the flow velocity of the jet on the circular cross-section, m/s; u_mp is the flow velocity of the jet on the inline section, m/s.

From Equations (10) and (11), it is obtained that the airflow velocity of the circular-section jet and the in-line jet is negatively correlated with the jet length when the initial velocity of the jet nozzle keeps the same. Suppose u_mc= u_mp=v_0, and substitute it into Equations (10) and (11), the expansion angle of the central section is generally a fixed value, i.e. ε=12°15′, the length of airflow core section L_{c0} and L_{p0} of circular section and inline nozzle will be

$$L_{c0} = 12.4\sqrt{\delta}r_0 - x_0 \tag{12}$$

$$L_{p0} = 14.4\sqrt{\delta}r_0 - x_0 \tag{13}$$

The momentum correction coefficient δ of the outlet section is a parameter to measure the uniformity of the gas velocity distribution. Here δ will be valued at 1. The velocity distribution is uniform since the air jet involved in this paper has no interference

from external factors, high temperature, high pressure, chemical reaction, etc. The distance from the jet pole to the mouth of the pipe x_0 is ignored since it is short, resulting from the much smaller diameter of the sprinkler than the transverse length of the gas field. When half of the characteristic length of the nozzle is 2 mm, the core length of the circular cross-section jet is about 24.8 mm, and the core length of the inline jet is about 28.8 mm. When comparing the flow velocity of the circular cross-section of the jet and that of the inline jet, u_{mc} is slightly smaller than ump. The inline jet core length is longer than the circular cross-section, which shows that the velocity of the circular cross-section jet is smaller when the distance is equal; that is, the velocity of the circular cross-section jet becomes significant with the distance decrease.

As the distance between the nozzle and the seed increases, air flow strength and air velocity reduce gradually. It is the airflow velocity that impacts the seed-clearing efficacy. Therefore, seed clearing distance is not a proper experimental index. To improve the efficiency of airflow utilization, it will be an effective way to ensure seeds are in the core section but leave a certain safe distance between the pipe mouth and seeds to prevent contact. Above all; the clearing distance is defined as 20 mm.

And the velocity of airflow at the mouth of the pipe is

$$v_0 = \frac{V_S}{A} \tag{14}$$

where, V_s is the volumetric flow of airflow, m^3/s; A is the area of the cross-section at the pipe mouth, m^2.

Therefore, in the study, it is necessary to ensure that the cross-sectional area of the circular sprinkler is equal to that of the inline nozzle, making the initial velocity comparable under the same force supply condition. However, the cross-section of the inline nozzle is a long and narrow rectangle. The characteristic length of the nozzle is smaller than that of the circular sprinkler when its cross-sectional area is equal. The jet velocity of the inline nozzle is much higher than that of the circular nozzle. Thus, the inline nozzle has a more robust seed-clearing capacity.

3.3 Study on the jet angle

In addition to the positive pressure airflow velocity, the positive pressure clearing airflow direction will also significantly affect the seed-clearing effect by changing the direction of the force exerted by the airflow on the seeds, thereby changing the stress state of the seeds. Figure 4 is the analysis of the stress state on seeds when the direction of the positive pressure airflow points to the center of the pinhole wheel (the positive pressure airflow is directly above the seed) and when the direction is at a certain angle with the center of the suction hole (the positive pressure airflow is obliquely above the seed).

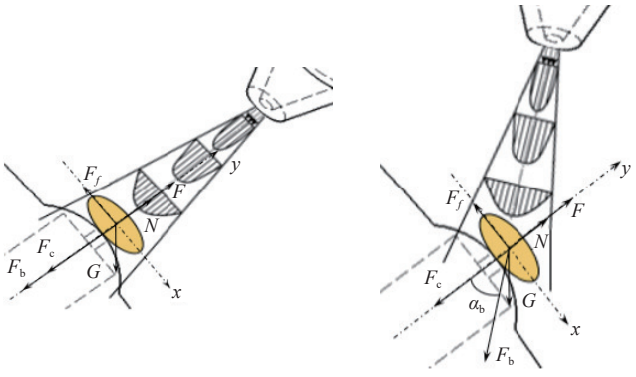

a. Positive upper barotropic flow b. Oblique upper barotropic flow

Note: F_f is the friction force of the pinhole wheel on seeds, N; N is the supporting force of the pinhole wheel on seeds, N; F is the centrifugal force on the seed, N; F_c is the absorption force of seed suction hole on seeds to maintain the seeds being absorbed, N; G is the gravity of seed, N; α_b is the angle of the line of airflow of seed clearing to the suction hole, (°).

Figure 4 Seed force state under positive airflow

It sets the direction of the adsorption force on the seeds to be the negative direction of the y-axis; when the positive pressure airflow is directly above the seeds, in the y-axis direction, the total of the adsorption force, the air blowing force, and the seed gravity balance with the support force and the centrifugal force from pinhole wheel on seeds. In the x-axis direction, it needs to be a balance between the friction force and vertical gravity. When airflow passes through the center of the pinhole wheel, the seeds' clearing capacity is relatively weak, and false clearing will be significantly reduced since seeds are not affected by shear forces in other directions.

The adsorption force and centrifugal force remain unchanged in the y direction. When the clearing pipe is at the oblique top, the air blowing force on the seeds in the y-axis direction decreases when the cleaning angle increases from 0° to α_b, with which the supporting force and the friction force on the seeds decrease as well; furthermore, as the clearing angle increases, making the airflow force larger and larger and the friction cannot be balanced, seeds will come out of the hole. Therefore, the seed clearing ability will increase with the increase of seed clearing angle α_b. At the same time, false clearing will increase significantly as the relatively more significant shear force clears the single seed with unstable adsorption out of the suction hole. The clearing angle is defined as 0°-45° because it is found in the pre-experiment that when the clearing angle α_b is greater than 45°, the leakage miss suction of the sowing device increases sharply, which cannot meet the test requirements. To prevent the cleared seeds from falling into the field and affecting the breeding experiment, the clearing air pipe should rotate counterclockwise to blow the cleared seeds back into the seeds hopper.

When the seed-cleaning air nozzle is moved to the top of the slant, the adsorption force and centrifugal force remain unchanged in the y-direction. When the seed cleaning angle is increased from 0° to α_b, the air-blowing force on the seeds in the y-axis direction decreases, decreasing the support and friction forces on the seeds. When the seed cleaning angle increases, it will lead to the air-blowing force in the x-direction becoming larger and larger until the friction force cannot be balanced, and the seeds will be separated from the type holes. Therefore, the seed clearing capacity increases with the seed clearing angle α_b increase. However, the more significant shear force will cause the single seeds not firmly adsorbed to be cleared out of the suction hole, and the probability of a false clearing phenomenon will increase significantly. Through the pre-experiment, it was found that the seed clearing angle α_b was greater than 45°, the seeding device seed leakage index increased sharply and could not meet the test requirements, so the selected clearing angle range was 0°-45°. To prevent the cleared seeds from falling into the field and affecting the breeding test, the seed-clearing air tube should be turned counterclockwise to use the wind to blow the cleared seeds back into the seed box.

In addition, the fan's negative pressure directly affects the suction hole's absorption force on the seeds. It determines the ability of the wheat seeds on the suction hole to resist the impact of airflow. Therefore, the negative supply pressure of the single-seed precision sowing device will also significantly affect the effectiveness of the seed-clearing operation.

4 Experiments

4.1 Experimental materials and equipment

A test bed was set up to study the effect of positive pressure airflow on seed clearing. A stable wind supply should be ensured since fans should be installed in the pneumatic pinhole wheeled plot single-seed precision sowing device. And small DC fan should be installed in each sowing unit, as is shown in Figure 5a. Wonsmart WS9290B-24-220-X300 high-pressure fan was selected as the negative-pressure fan. Wonsmart WS9250C-24-240-X200 fan supplied positive pressure airflow for clearing pipe and positive pressure port. The parameters of the two fans are listed in Table 1.

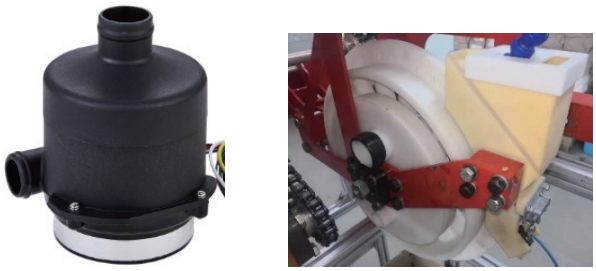

a. DC positive pressure fan b. Test prototype

Figure 5 Seed clearing test bench

Table 1 Fan parameters

Parameter/type	Negative pressure fan	Positive pressure fan
Normal voltage/V	24	24
Maximum air volume/$m^3 \cdot h^{-1}$	33	20
Maximum air volume/kPa	9	4.5
Current/A	8.3	5
Motor speed/$r \cdot min^{-1}$	27 000	24 000

Yannong 19, Bainong Aikang 58, and Tanmai 98, selected as the experimental wheat seeds, had little difference in the experimental results in the pre-experiment. Taking future 8000 low viscosity photosensitive resin as their material, The complex key components such as the pinhole wheel and pneumatic distribution center cover are processed by 3D printing technology. The frame and shaft are manufactured by the machining method. Figure 5b is the seed-clearing prototype for the test.

4.2 Single-factor test

The previous theoretical analysis found that factors such as the clearing angle, the shape of the nozzle, clearing air velocity, and negative pressure supply significantly influenced seed clearing. The orthogonal rotation test was adopted to obtain the best parameters of the operation. And a single-factor test is carried out to screen the best air pipe nozzle since the shape can barely be quantified. A universal bamboo-shaped air pipe, whose direction can be adjusted flexibly, was selected for the positive pressure seed-clearing mechanism. When the cross-sectional area radius of the air pipe outlet of the round nozzle is 2 mm, the inline nozzle, processed by 3D printing technology, with its cross-sectional area equal to that of the round nozzle, has a width equal to that of the seed suction boss, which is 14 mm, the slit width was calculated accordingly to be about 0.9 mm. Figure 6 is the air pipe nozzle.

The test conditions are as follows: seed clearing angle 0°, seed clearing air velocity 50 m/s, supply negative pressure 7.5 kPa. The seed leakage index, seed reabsorption index, and seed qualification index[38] were selected as evaluation indexes. The test was repeated three times, and at least 200 seed suction results were recorded. The average value of each index is listed in Table 2.

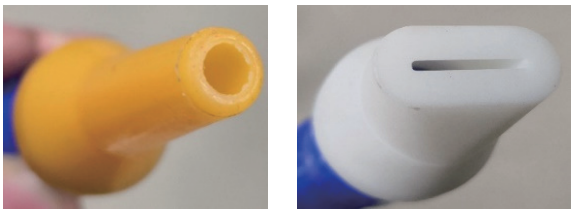

a. Circular shape b. Inline shape

Figure 6 Tracheal nozzle

Table 2 Single factor test results of nozzle shape

Factors/indicators	Circular sprinkler	Inline nozzle (horizontal)	Inline nozzle (vertical)
Seed leakage index/%	11.1	12.3	7.9
Seed reabsorption index/%	2.1	1.7	2.0
Seed qualification index /%	86.8	86	90.1

The evaluation criteria required the seed leakage index and seed reabsorption index to be smaller, if possible, and the seed qualification index to be more significant. As seen from the data in Table 1, the seed qualification index of the horizontal inline nozzle is the lowest. Still, the seed leakage index is the highest, indicating that the horizontal inline nozzle has a seed-clearing solid ability. In contrast, the tiny seed qualification index is because of the high probability of false clearing. The vertical inline nozzle performs best with optimal seed qualification and leakage index. Because it forms a longitudinal belt wind curtain, making the airflow velocity change in a gradient; that is, the airflow velocity when first contact with the seed is relatively low and increases gradually to the maximum at the midpoint of the wind curtain and then decreases gradually. This kind of air distribution helps improve seed-clearing efficiency. The index tested on the round nozzle is between the above two types of nozzles but is more similar to the horizontal inline nozzle. Therefore, the vertical inline nozzle with the best all-around performance is selected.

4.3 Orthogonal rotational test

To study the effects of seed clearing angle, seed air velocity, and supply negative pressure on seed clearing performance, the orthogonal rotation test of 3 factors and 5 levels was carried out. The upper limit of the clearing air velocity and the negative supply pressure is the measured value when the fan is at the maximum output, and the lower limit is the measured value when the fan is just enough to maintain its stable operation. The test factors and levels are listed in Table 3.

Table 3 Test factors and levels

Factor/level	Seed cleaning angle X_1/(°)	Cleaning airflow velocity X_2/$m \cdot s^{-1}$	Supply negative pressure X_3/kPa
Upper star arm (+γ)	0	20	5
To the upper level (+1)	9.12	32.16	6
Zero level (0)	22.5	50	7.5
Lower level (–1)	35.88	67.84	9
Lower star arm (-γ)	45	80	10

The self-lock function of the bamboo-shaped air pipe cannot help the positive pressure seed-clearing mechanism to ensure the accurate spatial position of the air pipe nozzle. Such factors as adjustment errors and machine vibration will change the seed clearing angle and distance. Therefore, a seed hopper cap with a slot at different angles to the horizontal surface to limit the air pipe can help locate the air pipe and ensure an accurate clearing distance. The seed hopper cap is shown in Figure 7.

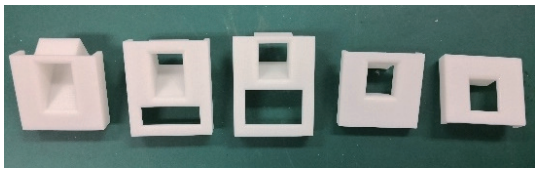

Figure 7 Seed box cover processing and installation

The test condition follows the pinhole wheel angular velocity of 2.31 rad/s, the operating speed of 1.5 km/h. The test is repeated three times. The test proposals and results are listed in Table 4.

Table 4 Experiment scheme and results

Test No.	Test factor			Performance index		
	X_1	X_2	X_3	Seed leakage index	Seed reabsorption index	Seed qualification index
1	1	1	1	6.1	5.2	88.7
2	1	1	–1	2.2	8.5	89.3
3	1	–1	1	21.8	0	78.2
4	1	–1	–1	9.8	1.1	89.1
5	–1	1	1	9.3	2.4	88.3
6	–1	1	–1	7.4	3.9	88.7
7	–1	–1	1	40.7	0	59.3
8	–1	–1	–1	19.2	0	80.8
9	1.682	0	0	7.9	3.3	88.8
10	–1.682	0	0	23.5	0	76.5
11	0	1.682	0	0.5	10.1	89.4
12	0	–1.682	0	27.5	0	72.5
13	0	0	1.682	21.8	0	78.2
14	0	0	–1.682	5.9	2.2	91.9
15	0	0	0	8.1	0.2	91.7
16	0	0	0	9.2	1.1	89.7
17	0	0	0	9.2	0.6	90.2
18	0	0	0	6.8	1.1	92.1
19	0	0	0	8.9	0.9	90.2
20	0	0	0	6.4	1	92.6
21	0	0	0	7.1	0.4	92.5
22	0	0	0	7.7	0.5	91.8
23	0	0	0	9.3	0.2	90.5

4.4 Test results analysis

4.4.1 Significance and interaction analysis of seed leakage index Y_1

Variance analysis was conducted to analyze the test results of seed leakage index Y_1. The results are listed in Table 5.

Table 5 Analysis of variance of leaked absorption index

Source of variation	Sum of squares	Degree of freedom	Mean square	F	p
Model	1911.67	9	212.41	100.27	< 0.0001***
X_1	290.03	1	290.03	136.91	< 0.0001***
X_2	917.01	1	917.01	432.89	< 0.0001***
X_3	319.35	1	319.35	150.75	< 0.0001***
X_1X_2	49.5	1	49.5	23.37	0.0003***
X_1X_3	7.03	1	7.03	3.32	0.0916
X_2X_3	95.91	1	95.91	45.28	< 0.0001***
X_1^2	109.35	1	109.35	51.62	< 0.0001***
X_2^2	64.99	1	64.99	30.68	< 0.0001***
X_3^2	61.62	1	61.62	29.09	0.0001***
Lost to poor	17.3	5	3.46	2.7	0.1017
error	10.24	8	1.28		

Note: *** very significant (p<0.001); ** significant (0.001<p<0.01); * less significant (0.01<p<0.05). The same as below.

The seed clearing angle, air flow velocity, and supply negative pressure greatly impact the seed leakage index. The influences of these factors showed a descending ordered as airflow velocity, supply negative pressure, and seed clearing angle. In interaction terms, the influence of X_1X_2 and X_2X_3 on the seed leakage index is highly significant. The quadratic term has a very significant effect on the seed leakage index. After removing the insignificant factors, the regression equation between each factor and the index is obtained as

$$Y_1 = 37.963 - 0.836X_1 + 0.569X_2 - 10.092X_3 + 0.01X_1X_2 - 0.131X_2X_3 + 0.015X_1^2 + 0.006X_2^2 + 0.891X_3^2 \quad (15)$$

The regression model is highly significant (p<0.001), and the determination coefficient of the model R^2 is 0.9822, indicating that the uniformity model gives an excellent fit and that the test error is relatively small, which shows that the regression equation makes sense. The mismatch test of the above regression equation shows that the mismatch difference is insignificant, proving that the optimal parameter can be calculated based on the regression equation. The response surface graphs of the effects on the seed leakage index of seed clearing angle, air flow velocity, and supply negative pressure are obtained by the software Design-Expert8.0.6 as is shown in Figure 8.

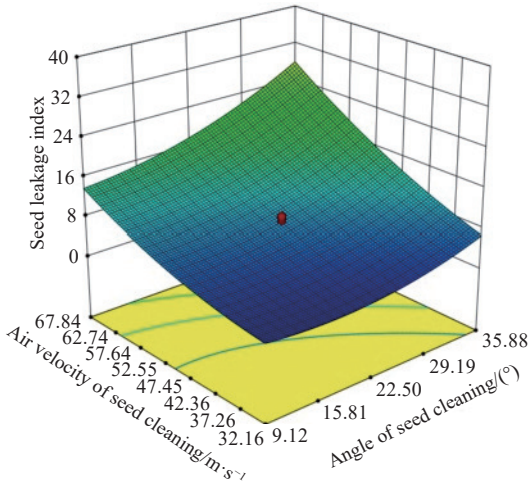

a. Angle of seed cleaning and air velocity of seed cleaning

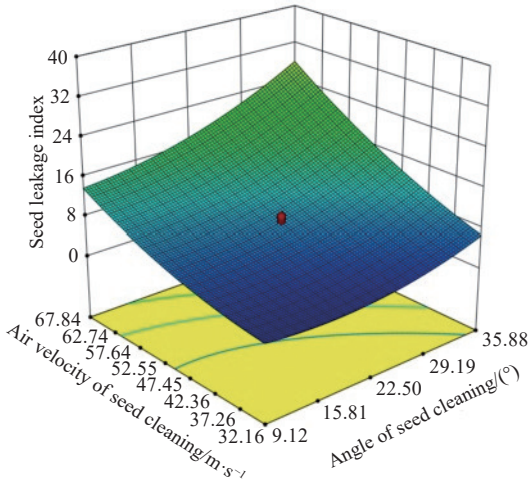

b. Air velocity of seed cleaning and negative supply pressure

Figure 8 Response surface of each factor to the seed leakage index

The interaction effect of seed clearing angle and airflow velocity on the seed leakage index is shown in Figure 8a. When the airflow velocity of seed clearing is fixed, the seed leakage index

increases with the increase of seed clearing angle, which shows that lateral shear force on seeds will increase when the seed clearing angle is too large. It will not only improve the seed clearing capacity but also make seeds that have been absorbed unable to resist the impact of positive airflow, resulting in a large number of false clearings, hence increasing the seed leakage index. However, the increase rate of the seed leakage index is not uniform; that is, it increases slowly when the seed clearing angle increases to 15° and increases more rapidly as the seed clearing angle keeps increasing, resulting in a rapid increase of seed leakage index. This shows that at the initial stage of the angle increase, the lateral shear on seeds is minimal, and the negative pressure in the suction hole is enough to maintain the adsorption state of the seed; that is to say, the positive pressure at a slight clearing angle on seeds will not change the adsorption state of a single-seed, making the seed leakage index remains stable in the early stage. With the increase of the lateral shear, the seed leakage index accelerates when the negative pressure is not enough to maintain the equilibrium. When the seed clearing angle is fixed, the seed leakage index increases gradually with the airflow velocity relatively uniformly, indicating that the seed clearing force and the probability of seed shedding increase as airflow velocity increases.

The interaction effect of cleaning airflow velocity and negative supply pressure on the seed leakage index is shown in Figure 8b. When the air velocity of seed clearing is fixed, the seed leakage index decreases with the increase of supply negative pressure. The increase of negative supply pressure is conducive to decreasing the seed leakage index by enhancing the resistant ability of seeds against positive air impact and maintaining seeds' adsorption. When the negative supply pressure is fixed, the seed leakage index increases with the increase of clearing airflow velocity.

4.4.2 Significance and interaction analysis of seed reabsorption index Y_2

Variance analysis was conducted to analyze the test results of seed reabsorption index Y_2. The results are listed in Table 6.

Table 6 Analysis of variance of respiration index

Source of variation	Sum of squares	Degree of freedom	Mean square	F	p
Model	162.45	9	18.05	91.48	<0.0001***
X_1	14.45	1	14.45	73.26	<0.0001***
X_2	94.3	1	94.3	477.93	<0.0001***
X_3	6.75	1	6.75	34.2	<0.0001***
X_1X_2	4.96	1	4.96	25.15	0.0002***
X_1X_3	1.05	1	1.05	5.33	0.0381*
X_2X_3	1.71	1	1.71	8.67	0.0114*
X_1^2	1.73	1	1.73	8.83	0.0108*
X_2^2	37.35	1	37.35	189.31	<0.0001***
X_3^2	0.3	1	0.3	1.5	0.2418
Misfit	1.48	5	0.3	2.2	0.1538
Error	1.08	8	0.14		

The three factors have an extremely significant influence on the seed reabsorption index. Their significance can be ordered as $X_2>X_1>X_3$. In the interaction items, the interaction of X_1X_2 is highly significant, and the interaction between X_1X_3 and X_2X_3 is less significant. In the quadratic term, X_1^2 had a significant effect on the seed reabsorption index, X_2^2 had a very significant effect, and X_3^2 had an insignificant effect. After removing the insignificant factors, the regression equation between each factor and the index is obtained as

$$Y_2 = 13.368 - 0.188X_1 - 0.572X_2 + 1.755X_3 + 0.003X_1X_2 - 0.018X_1X_3 - 0.017X_2X_3 + 0.002X_1^2 + 0.005X_2^2 \quad (16)$$

The regression model is highly significant (p<0.001) with a mismatch difference at 0.1538, which is not significant; the determination coefficient of the model R^2 is 0.9827, indicating that the uniformity model gives an excellent fit and that the test error is relatively small, which proves that the optimal parameter can be calculated based on the regression equation. The response surface graphs of the effects on seed reabsorption index of seed clearing angle, air flow velocity, and supply negative pressure are obtained, as shown in Figure 9.

The interaction effect of seed clearing angle and airflow velocity on the seed reabsorption index is shown in Figure 9a. When the airflow velocity of seed clearing is fixed, the seed reabsorption index decreases with the increase of seed clearing angle relatively uniformly, with no apparent stationary stage, indicating that the adsorption state of multiple seeds is less stable than that of single seeds. The appropriate external force will correct the multiple suction issue. When the clearing angle is fixed, the seed reabsorption index decreases with the increase of clearing airflow velocity. Starting at a relatively high value, its variation range is extensive, indicating that more than low clearing airflow velocity is needed to improve the multiple suction, resulting in a limited clearing efficiency. As a result, the seed reabsorption index is still high at this stage.

The interaction between the seed clearing angle and supply negative pressure is shown in Figure 9b. When the seed clearing angle is fixed, the seed reabsorption index increases with the increase of the supply negative pressure. As the negative pressure in the seed suction hole increases, the probability of re-seeding during seed pickup now leaves increases and places higher demands on the seed-clearing airflow. However, the magnitude of change is small and has less influence than the first two factors. When the supply negative pressure is fixed, the suction index decreases with the increase of the seed clearing angle.

The effect of the interaction between clearing air velocity and supply negative pressure is shown in Figure 9c. When the supply negative pressure is fixed, the seed reabsorption index decreases with the increase of clearing air velocity. When the airflow velocity is fixed, the seed reabsorption index increases with the increase of supply negative pressure.

In addition, there is a plane stage with a seed reabsorption index at 0 in some areas of the three response surfaces, indicating that with the change of parameters, seed clearing ability is continuously improved by eliminating the multiple suction. In contrast, the seed leakage index increases at the same time.

4.4.3 Significance and interaction analysis of seed qualification index Y_3

Variance analysis was conducted to analyze the test results of seed qualification index Y_3. The results are listed in Table 7.

The three factors have an extremely significant influence on the seed qualification index. Their significance can be ordered as $X_2>X_3>X_1$. In the interaction items, the interaction of X_1X_2 and X_2X_3 is highly significant, and the interaction of X_1X_3 is less significant. The quadratic terms had a significant effect on the seed qualification index. The regression equation between each factor and the index is obtained as

$$Y_3 = 53.217 + 0.671X_1 + 0.004X_2 + 8.204X_3 - 0.014X_1X_2 + 0.065X_1X_3 + 0.148X_2X_3 - 0.017X_1^2 - 0.011X_2^2 - 0.953X_3^2 \quad (17)$$

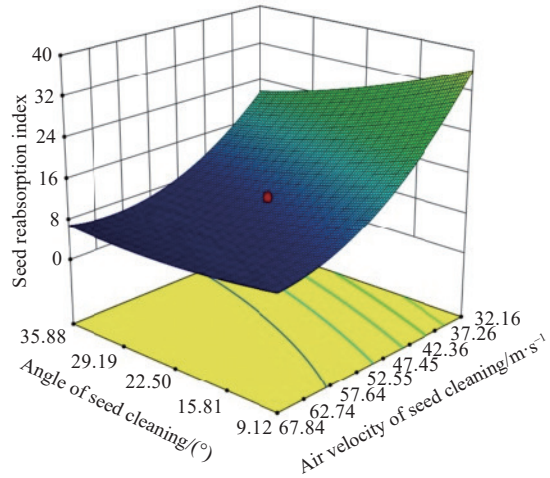

a. Angle of seed cleaning and air velocity of seed cleaning

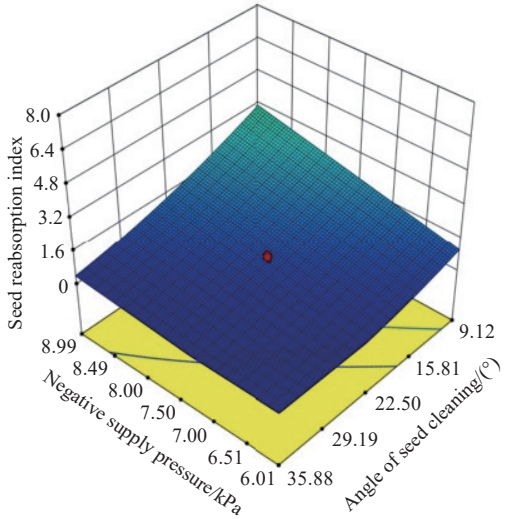

b. Angle of seed cleaning and negative supply pressure

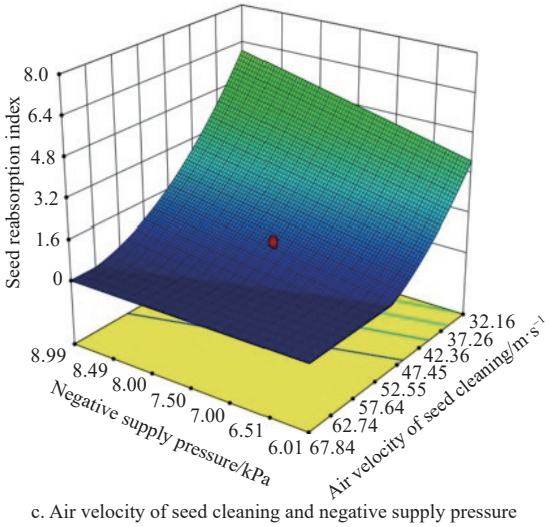

c. Air velocity of seed cleaning and negative supply pressure

Figure 9 Response surface of each factor to seed reabsorption index

The regression model is highly significant (p<0.001) with mismatch difference insignificant, and the determination coefficient of the model R^2 is 0.9813, indicating that the uniformity model gives an excellent fit and that the test error is relatively small, which proves that the regression equation makes sense. The response surface graphs of the effects on the seed qualification index of seed clearing angle, air flow velocity, and supply negative pressure are obtained, as shown in Figure 10.

Table 7 Seed qualification index analysis of variance

Source of variation	Sum of squares	Degree of freedom	Mean square	F	p
Model	1458.8	9	162.09	75.61	<0.0001***
X_1	174.99	1	174.99	81.63	<0.0001***
X_2	423.19	1	423.19	197.4	<0.0001***
X_3	233.26	1	233.26	108.81	<0.0001***
X_1X_2	85.8	1	85.8	40.03	<0.0001***
X_1X_3	13.52	1	13.52	6.31	0.026*
X_2X_3	123.25	1	123.25	57.49	<0.0001***
X_1^2	138.7	1	138.7	64.7	<0.0001***
X_2^2	200.87	1	200.87	93.7	<0.0001***
X_3^2	70.47	1	70.47	32.87	<0.0001***
Misfit	18.09	5	3.62	2.96	0.0837
Error	9.78	8	1.22		

The interaction effect of seed clearing angle and airflow velocity on the seed qualification index is shown in Figure 10a. When the seed clearing air flow velocity is fixed, the seed qualification index increases at first and then decreases with the increase of the seed clearing angle. The reason is that at the initial stage of the clearing angle increase, the seed clearing ability of positive pressure airflow increases gradually, resulting in a rebalance of seeds absorbed on the suction hole under the interference of airflow, clearing out the excess seeds that are not absorbed firmly and leaving only one dominant seed; and with the continuous increase of seed clearing angle, affected by excessive lateral shear force, single-seed absorbed on some seed suction holes fell off, resulting in a significant increase of seed leakage index and a decrease seed qualification index. When the seed clearing angle is fixed, the changing trend of the seed qualification index affected by airflow velocity was similar to that affected by the seed clearing angle, increasing at first and then decreasing.

The interaction between the seed clearing angle and supply negative pressure is shown in Figure 10b. When the seed clearing angle is fixed, the seed qualification index increases with the increase of supply negative pressure, but the growth slows down gradually with a slight reduction; when the negative supply pressure is fixed, with the increase of seed clearing angle, the seed qualification index increases at first and then decreases as well. The effect of the interaction between air velocity and supply negative pressure is shown in Figure 10c. When the negative supply pressure is fixed, the seed qualification index increases first and then decreases with the increase of cleaning gas velocity. When the airflow velocity is fixed, the seed qualification index increases with supply negative pressure.

4.5 Optimize constraint objective of seed clearing parameters based on a regression model

To obtain the best operation parameters for a single-seed precision sowing device, the optimization module of DesignExpert8.0.6 software was applied to optimize the constrained objective optimization solution of the above three regression models. The seed leakage index Y_1 and the seed reabsorption index Y_2 are taken as the constraint objective to calculate the seed qualification index because the seed qualification index is the level II index that was calculated based on the seed reabsorption index and the seed leakage index, which cannot be fitted perfectly by regression equation, resulting in conflicts when the three parameters are fitted synchronously.

The single-seed precision sowing device is designed to complete the sowing in the original seed period of wheat plot

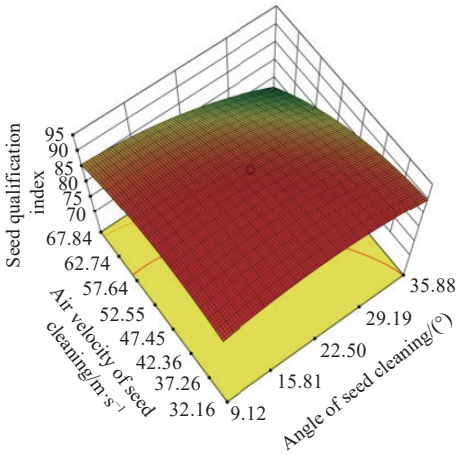

a. Angle of seed cleaning and air velocity of seed cleaning

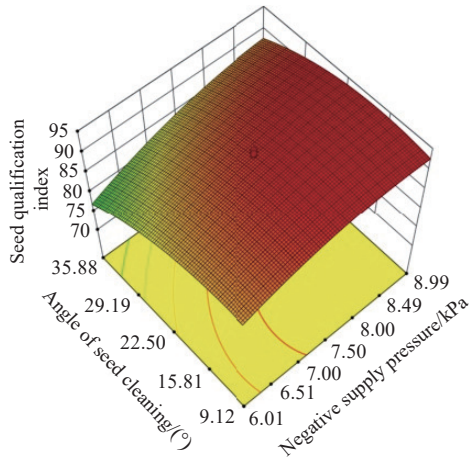

b. Angle of seed cleaning and negative supply pressure

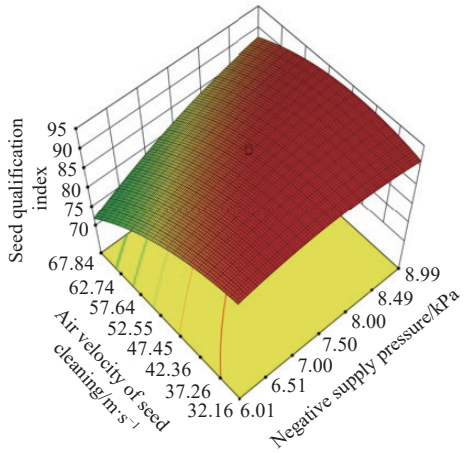

c. Negative supply pressure and air velocity of seed cleaning

Figure 10 Response surface of each factor to the seed qualification index

breeding. During this period, an investigation of the characteristics of a single wheat plant needs to be carried out. Multiple sowing is requested to be as minimum as possible and is set within 0.5% since it will significantly affect the growth and breeding trial. The seed leakage index should be optimized to a minimum as well. In addition, the greater the negative supply pressure, the greater the fan load and power consumption. The value of supply negative pressure should be reduced as much as possible when operation quality is stable. Thus, variables are added to set an upper limit for the supply negative pressure X_3. The final objective function is obtained as

$$\text{s.t.}\begin{cases}\text{Min } Y_1(X_1,X_2,X_3)\\ Y_2(X_1,X_2,X_3)\le 0.5\%\\ 0\le X_1\le 45\\ 20\le X_2\le 80\\ 5\le X_3\le a\end{cases} \tag{18}$$

where, a is the upper limit of supply negative pressure, kPa.

Different values of the upper limit of negative supply pressure are given in the value range of 5-10 kPa, and the optimal value of the seed leakage index under the condition of Equation (18) is obtained, as shown in Figure 11.

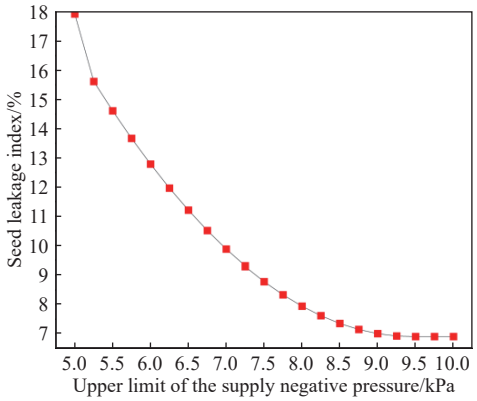

Figure 11 Relationship between the upper limit of the negative supply pressure and the optimal value of the seed leakage index

As seen from Figure 11, with the increase of the upper limit of negative supply pressure, the seed leakage index shows a downward trend that slows down obviously. When the upper limit of negative supply pressure reaches 8.5 kPa, the increase of negative supply pressure results in a limited increase in the seed leakage index. Therefore, 8.5 kPa is selected as the upper limit of supply negative pressure. Based on Equation (18), the following optimization results are calculated: the airflow velocity is 57.91 m/s when the clearing angle is 18.83°; the seed leakage index is 7.35%, the seed reabsorption index is 0.5%, and the seed qualification index is 92.15% when the negative supply pressure is 8.5 kPa.

To verify the accuracy of the regression equation, a rounding operation is conducted on the best parameters above. Thus, the clearing angle will be 19°, the airflow velocity will be 58 m/s, and the negative pressure will be 8.5 kPa. Under the above conditions, a verification test was carried out on the sowing test bed, repeated 3 times. The following test results were obtained from the test: the seed leakage index of 8.23%, the seed reabsorption index of 0.33%, and the seed qualification index of 91.44%, which was a minor difference from the optimization result, and met the design requirements[39]. Compared with the same type of positive and negative pressure precision seed planter (leakage rate of 3.47%, repeat rate of 3.83%), the leakage rate decreased significantly, and the repeat rate was high. However, a high seed reabsorption index is not acceptable for a plot breeding seeder. The designed wheat plot precision seeding device has better plot breeding seeding effect.

5 Conclusions

1) This study analyzed the force state of seeds subjected to seed cleaning airflow and determined that the critical factor affecting the magnitude of air blowing force on seeds is the velocity of seed cleaning airflow; explored the evolution law and airfield distribution after the airflow flowed out from the nozzle of the air

tube, and obtained the flow velocity distribution relationship of the overall section of the jet.

2) The analysis of the cross-sectional jet velocity was carried out for a typical nozzle shape. The mathematical models of the jet velocity in the circular and planar sections were established. The length of the core section of the circular jet was about 24.8 mm, and the length of the core section of the monoclinic jet was about 28.8 mm. The mechanical state of the seeds during seed cleaning in the *y*-axis and inclined directions was analyzed, and the seed cleaning capacity of the positive airflow increased with the increase of the seed cleaning angle.

3) The single-factor test found that the vertical inline nozzle had the best pass index, seed leakage index and overall performance. Two three factors and five levels of orthogonal rotation tests were conducted with the seed cleaning angle, seed cleaning airflow speed and negative supply pressure as factors, and the seed leakage index, seed reabsorption index and pass index as evaluation indexes. The experiment showed that three factors significantly influence the seed cleaning performance, and the most significant influence is the seed cleaning airspeed.

4) The regression equation between each factor and the index was established, and the optimal parameters of clearing species were obtained by optimizing the constraint objective. It was verified that the optimum operation effect could be obtained at the seed cleaning angle of 19°, the seed cleaning air velocity of 58 m/s and the negative supply pressure of 8.5 kPa, and the seed leakage index was 8.23%, the seed reabsorption index was 0.33%, and the seed qualification index was 91.44%, which satisfied the design requirements.

Acknowledgements

This research was funded by the National Natural Science Foundation of China (Grant No. 52175260), the China Agriculture Research System (Grant No. CARS-03), the Key Research and development plan of Hainan Province (Grant No. ZDYF2022XDNY184), Project of Scientific Research in Colleges and Universities of Hainan Province (Grant No. Hnky2022-93), Research Start-up Fund Project of Hainan University (Grant No. KYQD(ZR)-22036) and the authors wish to thank them for their generous financial assistance.

[References]

[1] Dong Y X, Physiological mechanism and cultivation techniques of high yield and efficiency winter-seeded spring wheat in Inner Mongolia, Doctoral thesis. Inner Mongolia, China: Inner Mongolia Agricultural University, 2020; 143p. (in Chinese)

[2] Xu Q M, Li H W, He J, Wang Q J, Lu C Y, Wang C L. Design and experiment of the self-propelled agricultural mobile platform for wheat seeding. Transactions of the CSAE, 2021; 37(14): 1–11. (in Chinese)

[3] Cheng X P, Li H W, Lu C Y, He J, Wang Q J, Wang C, et al. Parameter optimization and experiment of centrifugal seed dispenser in wheat plot drill. Transactions of the CSAE, 2019; 35(20): 1–9. (in Chinese)

[4] Cheng X P, Li H W, Wang Q J, He J, Lu C Y, Yang W. Design and experiment of wheat seeding control system in plot seeder. Transactions of the CSAM, 2019; 50(7): 30–38. (in Chinese)

[5] El-Kholy M M, Kamel R M. Development and evaluation of an innovative grain cart with a pneumatic conveyor. Heliyon, 2021; 7(11): e08461.

[6] Feng J M, Qian D Y, Feng Y H, Tao L H, Zhuo J Y, Qing F X. Optimal structure design and performance tests of seed metering device with fluted rollers for precision wheat seeding machine. IFAC Papers OnLine, 2018; 51(17): 509–514.

[7] Wang Y B, Li H W, Hu H N, He J, Wang Q J, Lu C Y, et al. A noncontact self-suction wheat shooting device for sustainable agriculture: A preliminary research. Computers and Electronics in Agriculture. 2022; 197. 106927. doi: 10.1016/j.compag.2022.106927.

[8] Xi X B, Gu C J, Shi Y J, Zhao Y, Zhang Y F, Zhang Q, et al. Design and experiment of no-tube seeder for wheat sowing. Soil and Tillage Research. 2020; 204: 104724. doi:10.1016/j.still.2020.104724.

[9] Liu J X, Wang Q J, Li H W, He J, Lu C Y. Design and seed suction performance of pinhole-tube wheat precision seeding device. Transactions of the CSAE, 2019; 35(11): 10–18. (in Chinese)

[10] Liu J X, Wang Q J, Li H W, He J, Lu C Y, Wang C. Numerical analysis and experiment on pneumatic loss characteristic of pinhole-tube wheat uniform seeding mechanism. Transactions of the CSAM, 2020; 51(6): 29–37. (in Chinese)

[11] Lai Q H, Sun K, Yu Q X, Qin W. Design and experiment of a six-row air-blowing centralized precision seed-metering device for Panax notoginseng. Int J Agric & Biol Eng, 2020; 13(2): 111–122.

[12] Liu W, Hu J P, Yao M J, Zhao J, Lakhiar I A, Lu C T, et al. Magnetic field distribution simulation and performance experiment of a magnetic seed-metering device based on the combined magnetic system. Int J Agric & Biol Eng, 2021; 14(1): 108–117.

[13] Wang G P, Sun W, Chen L D, Zhang H, Liu X L, Li H L, et al. Realization of an integrated seeding and compensating potato planter based on one-way clutch. Int J Agric & Biol Eng, 2020; 13(3): 79–87.

[14] Wang Y B, Li H W, Hu H N, He J, Wang Q J, Lu C Y, et al. DEM-CFD coupling simulation and optimization of a self-suction wheat shooting device. Powder Technology. 2021; 393: 494–509.

[15] Yang W. Research on technology and equipment of precision seeding in maize breeding. Doctoral thesis. Beijing, China: Chinese Academy of Agricultural Mechanization Sciences, 2019; 105p. (in Chinese)

[16] Introduction of machines and tools of Wintersteiger Company in Austria, 2021.https://www.nongjitong.com/company/wintersteiger/. Accessed on [2021-08-03] (in Chinese)

[17] Yang W, Fang X F, Li J D, Li L X. Design and experiment of air-suction precision seed meter with self-clearing seed chamber for corn plot test. Transactions of the CSAM, 2019; 50(6): 64–73. (in Chinese)

[18] Zhang L Y. Design on wheat hill-drop planter based on PLC controlled used for experimental plot. MS dissertation, Tai'an: Shandong Agricultural University, 2012; 64p. (in Chinese)

[19] Zhang D D. Improving design and test on pneumatic hill-drop planter for wheat breeding plot. MS dissertation. Tai'an: Shandong Agricultural University, 2014; 58 p. (in Chinese)

[20] Liu Y Q. Experimental study on air-suction drum-type vegetable seedling seeder. Beijing: Chinese Academy of Agricultural Mechanization Sciences, 2018; 69p. (in Chinese)

[21] Liu Y Q, Zhao Z B, Liu L J, Zhao J H, Wang J Y. Research status and development trend of vegetable plug seedling seeder. Agricultural Engineering, 2018; 8(1): 6–12. (in Chinese)

[22] Liu Y Q, Liu L J, Zhao Z B, Zhao J H, Cui W. Design and experiment on plant seedling device for vegetable seedling seeder. Transactions of the CSAM, 2018; 49(S1): 83–91. (in Chinese)

[23] Zhang K. Study on mechanism and parameters of air suction cylinder type precise seeding device for maize with plant material bowl-tray. Doctoral thesis. Daqing, China: Heilongjiang Bayi Agricultural Reclamation University, 2018;124p. (in Chinese)

[24] Zhang K, Yi S J. Simulation and experimental optimization on filling seeds performance of seed metering device with roller of air-suction. Transactions of the CSAM, 2017; 48(7): 78–86. (in Chinese)

[25] Xu G J. Design and experiment of pneumatic cylinder array precision seed-metering device for cotton. Master dissertation. Shihezi: Shihezi University, 2018; 64p. (in Chinese)

[26] Ni X D, Xu G J, Wang Q, Peng X R, Wang J, Hu B. Design and experiment of pneumatic cylinder array precision seed-metering device for cotton. Transactions of the CSAM, 2017; 48(12): 58–67. (in Chinese)

[27] Wen Q, Sha J, Liu Y Z. TR-PIV Measurement of the turbulent submerged jet and pod analysis of the dynamic structure. Journal of Experiments in Fluid Mechanics, 2014; 28(4): 16–24. (in Chinese)

[28] Cai Y T. Numerical simulation of air resistance of light materials. MS dissertation. Qinhuangdao; Yanshan University, 2021; 77p. (in Chinese)

[29] Dun G Q, Mao N, Gao Z Y, Wu X P, Liu W H, Zhou C. Model construction of soybean average diameter and hole parameters of seed-metering wheel based on DEM. Int J Agric & Biol Eng, 2022; 15(1): 101–110.

[30] Han D D, Zhang D X, Jing H, Yang L, Cui T, Ding Y Q, et al. DEM-CFD coupling simulation and optimization of an inside-filling air-blowing maize

precision seed-metering device. Computers and Electronics in Agriculture, 2018; 150: 426–438.

[31] Liang Y Q, Tang Z, Zhang H, Li Y M, Ding Z, Su Z. Cross flow fan on multi-dimensional airflow field of air screen cleaning system for rice grain. Int J Agric & Biol Eng, 2022; 15(4): 223–235.

[32] Lei X L, Liao Y T, Liao Q G. Simulation of seed motion in seed feeding device with DEM-CFD coupling approach for rapeseed and wheat. Computers and Electronics in Agriculture, 2016; 131: 29–39.

[33] Patel M, Thomas J, Joshi H C. Flow characterization of supersonic gas jets: Experiments and simulations. Vacuum, 2021; 192: 110440.

[34] Gahlot N K, Singh N K. Effect of air jet with injection pressure on the performance of mixed compression air intake. Proceedings of the Institution of Mechanical Engineers, Part G: Journal of Aerospace Engineering, 2020; 235(9). doi:10.1177/0954410020966507.

[35] Pimshtein V G. On the structure of the sound field near a turbulent jet emanating from a nozzle in the case where perturbations exist in its prechamber. Journal of Engineering Physics and Thermophysics, 2021; 94(3): 666–669.

[36] He R Y, Wang J L, Xu G M, He X Y, Duan P F. Design and experiment of wheat precise seed metering apparatus with positive and negative pressure with function of limiting seed filling posture. Transactions of the CSAM, 2022; 53(9): 39–49, 167. (in Chinese)

[37] Zhao C Q, Jiang Y. Gas jet dynamics. Beijing: Beijing Institute of Technology Press, 1998. (in Chinese)

[38] GB/T6973-2005 Inspection and Quarantine of the People's Republic of China (AQSIQ). Test method for single grain (precision) seeder, 2005. (in Chinese)

[39] JB/T10293-2013. Enterprise Standard of Shenyang Tianhe Xingda Machinery Manufacturing Co., Ltd. Test method for single grain (precision) seeder, 2013. (in Chinese)